



Generalized Darboux transformation and solitons for a Kraenkel-Manna-Merle system in a ferromagnetic saturator

Xi-Hu Wu · Yi-Tian Gao · Xin Yu · Fei-Yan Liu

Received: 9 December 2022 / Accepted: 13 April 2023 / Published online: 6 June 2023
© The Author(s), under exclusive licence to Springer Nature B.V. 2023

Abstract Ferromagnetic materials are considered to have the applications in data storage, data processing and telecommunication. A Kraenkel-Manna-Merle system, which describes the nonlinear electromagnetic short waves in a ferromagnetic saturator, is investigated in this paper. With respect to the magnetization related to the saturated ferromagnetic material and external magnetic field, a generalized Darboux transformation (GDT) is constructed and utilized to derive the solitons, multi-pole solitons and their interactions. Analytic expressions of the double-pole solitons are offered and analyzed via the asymptotic analysis. Then, amplitudes, characteristic lines, slopes and phase shifts of the asymptotic solitons are presented. With the multiple spectral parameters involved in the GDT, interactions among the solitons and multi-pole solitons are illustrated.

Keywords Ferromagnetic material · Kraenkel-Manna-Merle system · Generalized Darboux transformation · Multi-pole soliton · Asymptotic analysis

1 Introduction

Recent development of the computer and information technology has accompanied the demands of the massive data and high-density storage [1]. Ferromagnetic materials have been regarded as the ideal storage media in information technology [2, 3]. Ferromagnetic materials, e.g., iron, cobalt, nickel and certain rare-earth metals, have exhibited a spontaneous net magnetization at the atomic level in the absence of an external magnetic field [4]. Furthermore, ferromagnetic materials have been considered to have the applications in data processing and telecommunication [5, 6].

To describe the nonlinear electromagnetic short waves in a ferromagnetic saturator, a Kraenkel-Manna-Merle system has been proposed¹ [7–23]

X.-H. Wu · Y.-T. Gao (✉) · X. Yu (✉) · F.-Y. Liu
Ministry-of-Education Key Laboratory of Fluid
Mechanics and National Laboratory for Computational
Fluid Dynamics, Beijing University of Aeronautics and
Astronautics, Beijing 100191, China

Y.-T. Gao
e-mail: gaoyt163@163.com

X. Yu
e-mail: yuxin@buaa.edu.cn

X.-H. Wu
Shen Yuan Honors College, Beijing University of
Aeronautics and Astronautics, Beijing 100191, China

¹ According to Ref. [7], the researchers have thought the ferromagnetic saturator as a insulator, i.e., a ferromagnetic saturator with the zero conductivity. During the derivation of System (1), effects of the current and free charge have been ignored in the Maxwell equation [7].

$$\begin{aligned} u_{xt} - uv_x + \kappa v_x &= 0, \\ v_{xt} + uu_x &= 0, \end{aligned} \quad (1)$$

where u and v are two real differentiable functions of x and t , u is related to the component of the magnetization in a certain direction about the saturated ferromagnetic material, v is related to the component of the external magnetic field in a certain direction, κ represents the damping effect, and the subscripts denote the partial derivatives with respect to the scaled space variable x and time variable t .

Solitons, a kind of the nonlinear waves, have exhibited the capability of the propagation of the waves without losing the shape for a long distance [24]. Therefore, solitons, which are stable, has been investigated in fluid mechanics [25], fiber optics [26], plasma physics [27], material sciences [28] and other fields [29]. With the development of the advanced large-scale information storage and transmission, solitons have shown the potential applications in ferromagnetic materials [30]. Moreover, other nonlinear waves, e.g., breathers, periodic waves and rogue waves, have also attracted the researchers' attention [31–34].

For System (1), the breather solitons, periodic oscillation solitons and multi-pole instantons via the consistent tanh expansion method have been presented [8]; certain dark solitons, bright solitons, singular solitons, combined dark-bright solitons, combined dark-singular solitons, periodic and singular periodic waves via the extended sinh-Gordon equation expansion method have been exhibited [9]; loop-like periodic waves in the Jacobi elliptic functions and solitons in the hyperbolic functions have been investigated [10]; effects of the inhomogeneous exchange and simultaneous damping effects on the magnetic solitons have been explored [11]; loop solitons in the localized multivalued waveguide channels have been offered [12]; certain solitons have been studied via the inverse scattering transform method and Wadati-Konno-Ichikawa scheme [13]; Darboux transformation (DT) and a series of the loop-like soliton structures have been obtained [14]; through the generalized G'/G -expansion method, hump-soliton, cusp-soliton, loop-soliton and kink-soliton have been observed [15]; single soliton, complex combo solitons, complex hyperbolic and trigonometric solutions through the extended direct algebraic method have been studied [16]; two types of the soliton twining behaviors have been derived via the bilinear method [17]; two

types of the periodically oscillating solitons have been discussed via the Riccati equation mapping method [18]; influences of the damping effect on the solitons in the ferrites materials have been investigated [19, 20]; some novel traveling wave solutions have been presented [21]; certain dark, singular and combo solitons along with periodic solutions have been studied via the modified auxiliary equation method and generalized projective Riccati equations method [22]; oscillation rogue waves via the truncated Painleve method have been obtained [23].

When κ is selected as 0, a Lax pair for System (1) has been obtained as [14, 35]

$$\begin{aligned} \Phi &= (\phi_1 \quad \phi_2)^T, \quad \Phi_x = U\Phi, \quad \Phi_t = V\Phi, \\ U &= \lambda \begin{pmatrix} v_x & u_x \\ u_x & -v_x \end{pmatrix}, \quad V = \begin{pmatrix} \frac{1}{4\lambda} & -\frac{u}{2} \\ \frac{u}{2} & -\frac{1}{4\lambda} \end{pmatrix}, \end{aligned} \quad (2)$$

where ϕ_1 and ϕ_2 are two real differentiable functions of x and t , λ is a real spectral parameter, the superscript “T” denotes the transpose of the matrix. From the compatibility condition $U_t - V_x + UV - VU = 0$ of Lax Pair (2), System (1) has been obtained [14].

DT method has enabled the users to obtain the solutions with the aid of the Lax pair of certain nonlinear evolution equations [36]. However, one limitation of the DT method has been considered as that each spectral parameter can only be iterated once in the multi-iteration process [36]. Thus, in the N -fold solutions obtained via the DT, each spectral parameter has corresponded to a separate localized wave component, e.g., the soliton, breather and rogue wave, where N is a positive integer [37]. On the basis of Lax Pair (2), N -fold DT and solitons with the straight characteristic lines for System (1) have been offered [35]. However, due to the disturbances and soliton energy dissipations in the ferromagnetic saturator, velocities of the nonlinear waves for System (1) have been considered as changeable under certain conditions [7]. Therefore, we have considered that the localized waves with the changeable velocities have the potential applications in the ferrites.

Multi-pole solitons, also called the degenerate solitons or higher-order solitons, whose characteristic lines are the curves, have been obtained through the generalized Darboux transformation (GDT) method and Hirota method [38–40]. Multi-pole solitons have

described the interactions of multiple chirped pulses with the same amplitudes and group velocities in an optical fiber [41]. Different from the DT method, GDT method, in which the spectral parameters can be iterated more than once, has enabled us to obtain the localized waves with the changeable velocities [42]. In the GDT method, the k th-order multi-pole solitons have been derived through iterating one spectral parameter k times, which are different from the k th-order solitons obtained via the Darboux transformation (DT) method, where k is a integer and $k \geq 2$ [43].

To our knowledge, GDT, multi-pole solitons and interaction among the solitons and multi-pole solitons for System (1) have not been investigated. In Sect. 2,

$$a^{(1)} = \frac{\Gamma_1}{\Gamma}, \quad b^{(1)} = \frac{\Gamma_2}{\Gamma},$$

$$\Gamma = \begin{vmatrix} \lambda_1 \phi_{1,1} & \lambda_1^2 \phi_{1,1} & \cdots & \lambda_1^N \phi_{1,1} & \lambda_1 \phi_{2,1} & \lambda_1^2 \phi_{2,1} & \cdots & \lambda_1^N \phi_{2,1} \\ (-1)^1 \lambda_1 \phi_{2,1} & (-1)^2 \lambda_1^2 \phi_{2,1} & \cdots & (-1)^N \lambda_1^N \phi_{2,1} & (-1)^2 \lambda_1 \phi_{1,1} & (-1)^3 \lambda_1^2 \phi_{1,1} & \cdots & (-1)^{N+1} \lambda_1^N \phi_{1,1} \\ \lambda_2 \phi_{1,2} & \lambda_2^2 \phi_{1,2} & \cdots & \lambda_2^N \phi_{1,2} & \lambda_2 \phi_{2,2} & \lambda_2^2 \phi_{2,2} & \cdots & \lambda_2^N \phi_{2,2} \\ (-1)^1 \lambda_2 \phi_{2,2} & (-1)^2 \lambda_2^2 \phi_{2,2} & \cdots & (-1)^N \lambda_2^N \phi_{2,2} & (-1)^2 \lambda_2 \phi_{1,2} & (-1)^3 \lambda_2^2 \phi_{1,2} & \cdots & (-1)^{N+1} \lambda_2^N \phi_{1,2} \\ \vdots & \vdots & \ddots & \vdots & \vdots & \vdots & \ddots & \vdots \\ \lambda_N \phi_{1,N} & \lambda_N^2 \phi_{1,N} & \cdots & \lambda_N^N \phi_{1,N} & \lambda_N \phi_{2,N} & \lambda_N^2 \phi_{2,N} & \cdots & \lambda_N^N \phi_{2,N} \\ (-1)^1 \lambda_N \phi_{2,N} & (-1)^2 \lambda_N^2 \phi_{2,N} & \cdots & (-1)^N \lambda_N^N \phi_{2,N} & (-1)^2 \lambda_N \phi_{1,N} & (-1)^3 \lambda_N^2 \phi_{1,N} & \cdots & (-1)^{N+1} \lambda_N^N \phi_{1,N} \end{vmatrix},$$

$$\gamma = (-\phi_{1,1}, -\phi_{2,1}, -\phi_{1,2}, -\phi_{2,2}, \dots, -\phi_{1,N}, -\phi_{2,N})^T, \tag{5}$$

with symbolic computation [44–48] we will construct a GDT for System (1). In Sect. 3, multi-pole solitons and interaction among the solitons and multi-pole solitons for System (1) will be presented and analyzed. In Sect. 4, our conclusions will be drawn.

2 GDT for System (1)

Based on Lax Pair (2), we firstly construct of an N -fold Darboux transformation for System (1). Motivated by the form of the first-order DT matrix in Refs. [14, 35], we assume the N -fold DT matrix $D^{[N]}$ as the following form

$$D^{[N]} = \begin{pmatrix} 1 + \sum_{j=1}^N a^{(j)} \lambda^j & \sum_{j=1}^N b^{(j)} \lambda^j \\ \sum_{j=1}^N (-1)^{j+1} b^{(j)} \lambda^j & 1 + \sum_{j=1}^N (-1)^j a^{(j)} \lambda^j \end{pmatrix}, \tag{3}$$

where $j = 1, 2, \dots, N$, $a^{(j)}$'s and $b^{(j)}$'s are $2N$ functions of x and t to be determined, and the superscript $[N]$ denotes the N th-order iteration.

Through the following equations [35]

$$\left(D^{[N]} \Phi \right) \Big|_{\lambda=\lambda_j} = 0, \tag{4}$$

we utilized the Cramer's Rule and calculate $a^{(1)}$ and $b^{(1)}$ as

where Γ_1 is derived through replacing the first column of Γ with γ , Γ_2 is derived through replacing the $(N + 1)$ th column of Γ with γ , λ_j 's are N different spectral parameters, and $(\phi_{1,j}, \phi_{2,j})^T$ is a solution of Lax Pair (2) at $\lambda = \lambda_j$ and the seed solutions u, v .

Then, an N -fold DT and solutions for System (1) can be expressed as

$$\Phi^{[N]} = D^{[N]} \Phi, \quad \Phi_x^{[N]} = U^{[N]} \Phi^{[N]}, \quad \Phi_t^{[N]} = V^{[N]} \Phi^{[N]},$$

$$U^{[N]} = \lambda \begin{pmatrix} v_x^{[N]} & u_x^{[N]} \\ u_x^{[N]} & -v_x^{[N]} \end{pmatrix}, \quad V^{[N]} = \begin{pmatrix} \frac{1}{4\lambda} & -\frac{u^{[N]}}{2} \\ \frac{u^{[N]}}{2} & -\frac{1}{4\lambda} \end{pmatrix},$$

$$u^{[N]} = u + b^{(1)}, \quad v^{[N]} = v + a^{(1)} + f_1(t), \tag{6}$$

where $f_1(t)$ is a differential function of t , u and v are the seed solutions, $u^{[N]}$ and $v^{[N]}$ are the N -fold solutions, and $U^{[N]}$ and $V^{[N]}$ are the transformed Lax pair matrices.

Next, on the basis of N -Fold DT (6), we will construct a GDT for System (1).

We choose M spectral parameters λ_s , where M is a positive integer, $M \leq N$ and $s = 1, 2, \dots, M$. Among the M spectral parameters, each spectral parameter λ_s will be iterated $r_s + 1$ times, where r_s is a positive integer and $M + \sum_{s=1}^M r_s = N$. We add a real small parameter perturbation ϵ to λ_s , i.e.,

$$\lambda_s \rightarrow \lambda_s + \epsilon. \tag{7}$$

At this time, the relationships between the potentials $u^{[N]}$, $v^{[N]}$ and u , v via the GDT is the same as the relationships in N -Fold DT (6). However, different from Eq. (4), $a^{(j)}$'s and $b^{(j)}$'s are determined via the following equations

$$\lim_{\epsilon \rightarrow 0} D^{[N]} \Big|_{\lambda=\lambda_s+\epsilon} \begin{pmatrix} \phi_1 \\ \phi_2 \end{pmatrix} \Big|_{\lambda=\lambda_s+\epsilon} \epsilon^{-p_s} = 0, \tag{8}$$

where $p_s = 0, 1, \dots, r_s$.

Through Eq. (8), $a^{(1)}$ and $b^{(1)}$ are determined as

$$u^{[N]} = u + b^{(1)}, \quad v^{[N]} = v + a^{(1)} + f_1(t),$$

$$a^{(1)} = \frac{|\Omega_1|}{|\Omega|}, \quad b^{(1)} = \frac{|\Omega_2|}{|\Omega|},$$

$$\Omega = \lim_{\epsilon \rightarrow 0} \left(A_1^T, \frac{d}{d\lambda_1} A_1^T, \dots, \frac{d^{r_1}}{(r_1)! d\lambda_1^{r_1}} A_1^T, \dots, A_m^T, \frac{d}{d\lambda_m} A_m^T, \dots, \frac{d^{r_M}}{(r_M)! d\lambda_M^{r_M}} A_M^T \right)^T,$$

$$A_s = (A_{s,1}, A_{s,2}), \tag{9}$$

$$A_{s,1} = \begin{pmatrix} (\lambda_s + \epsilon)\phi_1|_{\lambda=\lambda_s+\epsilon} & (\lambda_s + \epsilon)^2\phi_1|_{\lambda=\lambda_s+\epsilon} & \cdots & (\lambda_s + \epsilon)^N\phi_1|_{\lambda=\lambda_s+\epsilon} \\ (-1)^1(\lambda_s + \epsilon)\phi_2|_{\lambda=\lambda_s+\epsilon} & (-1)^2(\lambda_s + \epsilon)^2\phi_2|_{\lambda=\lambda_s+\epsilon} & \cdots & (-1)^N(\lambda_s + \epsilon)^N\phi_2|_{\lambda=\lambda_s+\epsilon} \end{pmatrix},$$

$$A_{s,2} = \begin{pmatrix} (\lambda_s + \epsilon)\phi_2|_{\lambda=\lambda_s+\epsilon} & (\lambda_s + \epsilon)^2\phi_2|_{\lambda=\lambda_s+\epsilon} & \cdots & (\lambda_s + \epsilon)^N\phi_2|_{\lambda=\lambda_s+\epsilon} \\ (-1)^2(\lambda_s + \epsilon)\phi_1|_{\lambda=\lambda_s+\epsilon} & (-1)^3(\lambda_s + \epsilon)^2\phi_1|_{\lambda=\lambda_s+\epsilon} & \cdots & (-1)^{N+1}(\lambda_s + \epsilon)^N\phi_1|_{\lambda=\lambda_s+\epsilon} \end{pmatrix},$$

where Ω_1 and Ω_2 can be obtained through replacing the 1st and $(N + 1)$ th columns of A_s in Ω with $(-\phi_1|_{\lambda=\lambda_s+\epsilon}, -\phi_2|_{\lambda=\lambda_s+\epsilon})^T$, respectively.

In particular, when $M = N$, i.e., $r_s = 0$, each of the N spectral parameters is iterated only once. Under such condition, Solutions (9) are reduced to the solutions in Eq. (5).

In Solutions (9), the value of M represents that Solutions (9) are composed of the M independent nonlinear waves, the value of r_s represents that the order of the nonlinear waves corresponding to λ_s is $r_s + 1$, and the value of N represents the total order of Solutions (9). In sum, N -Fold DT Matrix (3) and Solutions (9) form an N -Fold GDT for Eq. (1).

3 Solitonic interactions for System (1)

In order to derive certain solitons for System (1), we need to select the seed solutions for System (1). After the calculation, we find that the following seed solutions, i.e., $u = \alpha$, $v = \beta x + f_2(t)$, are the sufficient conditions for obtaining the solitons for System (1). In this section, we set $\alpha = f_2(t) = f_1(t) = 0$. However, the following studies can be extended to the cases under $\alpha f_1(t) f_2(t) \neq 0$.

Therefore, eigenfunction $\Phi(\lambda_s + \epsilon)$ with $\lambda = \lambda_s + \epsilon$ for Lax Pair (2) can be presented as

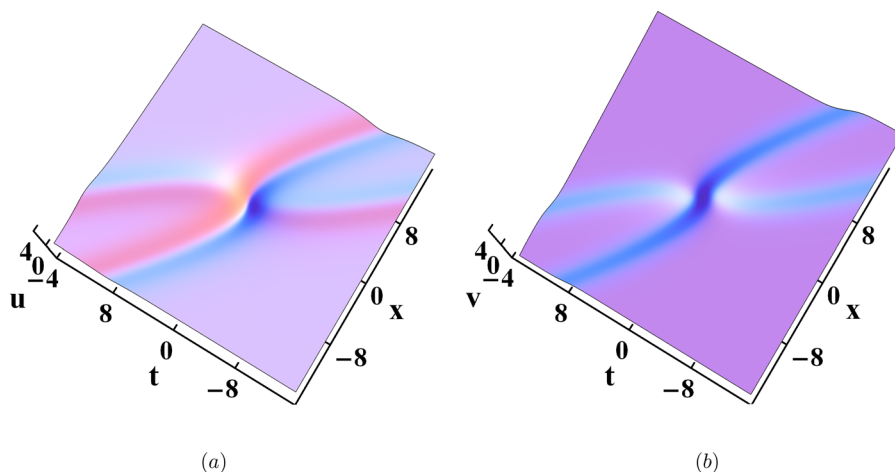
$$\Phi(\lambda_s + \epsilon) = \begin{pmatrix} g_s \\ h_s \end{pmatrix} = \begin{pmatrix} l_1 e^{\beta(\lambda_s + \epsilon)x + \frac{1}{4(\lambda_s + \epsilon)t}} \\ l_2 e^{-\beta(\lambda_s + \epsilon)x - \frac{1}{4(\lambda_s + \epsilon)t}} \end{pmatrix}, \tag{10}$$

where ϵ is a small parameter. Next, we expand eigenfunction $\Phi(\lambda_s + \epsilon)$ with the small parameter ϵ as follows:

$$\begin{aligned} \begin{pmatrix} g_s \\ h_s \end{pmatrix} &= \begin{pmatrix} g_{s,0} \\ h_{s,0} \end{pmatrix} + \begin{pmatrix} g_{s,1} \\ h_{s,1} \end{pmatrix} \epsilon + \begin{pmatrix} g_{s,2} \\ h_{s,2} \end{pmatrix} \epsilon^2 + \dots, \\ \begin{pmatrix} g_{s,0} \\ h_{s,0} \end{pmatrix} &= \begin{pmatrix} l_1 e^{\beta\lambda_s x + \frac{1}{4\lambda_s t}} \\ l_2 e^{-\beta\lambda_s x - \frac{1}{4\lambda_s t}} \end{pmatrix}, \quad \begin{pmatrix} g_{s,1} \\ h_{s,1} \end{pmatrix} = \begin{pmatrix} \left(\beta x - \frac{t}{4\lambda_s^2}\right) g_{s,0} \\ \left(\frac{t}{4\lambda_s^2} - \beta x\right) h_{s,0} \end{pmatrix}, \\ \begin{pmatrix} g_{s,2} \\ h_{s,2} \end{pmatrix} &= \begin{pmatrix} \left[\frac{1}{2}\left(\beta x - \frac{t}{4\lambda_s^2}\right)^2 + \frac{t}{4\lambda_s^3}\right] g_{s,0} \\ \left[\frac{1}{2}\left(\beta x - \frac{t}{4\lambda_s^2}\right)^2 - \frac{t}{4\lambda_s^3}\right] h_{s,0} \end{pmatrix} \dots \end{aligned} \tag{11}$$

We find that $g_{s,1}$, $h_{s,1}$, $g_{s,2}$, $h_{s,2}$ and so on are the mixtures of polynomials and exponential functions. Therefore, Solutions (9), which contain both the polynomials and exponential functions, are called the semirational solutions. Through setting the values of N , M and r_s in Solutions (9), different types of the semirational solutions for System (1) can be obtained. When $r_s \geq 1$, i.e., the complex spectral parameter λ_s is iterated more than once, λ_s corresponds to the $(r_s + 1)$ th-order multi-pole solitons in Solutions (9); when $r_s = 0$, λ_s corresponds to the one soliton in Solutions (9).

Fig. 1 3D figures of the double-pole solitons: **a** Component u ; **b** Component v via Solutions (12) with $\lambda_1 = 1$, $\beta = \frac{1}{4}$ and $l_{11} = l_{12} = 1$



3.1 Multi-pole solitons for Eq. (1)

As we set $M = r_1 = 1$, $N = 2$ in Solutions (9), with respect to the magnetization related to the saturated ferromagnetic material and external magnetic field, the double-pole solitons solutions for Eq. (1) can be derived as

$$\begin{aligned} u^{[1]} &= 2l_1 l_2 \frac{l_1^2(\rho - 2\lambda_1)e^{\frac{\theta}{2}} - l_2^2(\rho + 2\lambda_1)e^{-\frac{\theta}{2}}}{\lambda_1^2(l_1^4 e^{\theta} + l_2^4 e^{-\theta}) + l_1^2 l_2^2(\rho^2 + 2\lambda_1^2)}, \\ v^{[1]} &= \beta x - 2 \frac{\lambda_1(l_1^4 e^{\theta} - l_2^4 e^{-\theta}) + 2l_1^2 l_2^2 \rho}{\lambda_1^2(l_1^4 e^{\theta} + l_2^4 e^{-\theta}) + l_1^2 l_2^2(\rho^2 + 2\lambda_1^2)}, \\ \theta &= \frac{t}{\lambda_1} + 4\beta\lambda_1 x, \quad \rho = t - 4\beta\lambda_1^2 x. \end{aligned} \tag{12}$$

As shown in Fig. 1, the characteristic lines of the double-pole solitons are the curves. We also find that the background plane of $u^{[1]}$ is fixed, while the background plane of $v^{[1]}$ changes from negative to zero and then to positive with the increase of t .

Since the background of $u^{[1]}$ is fixed while the background plane of $v^{[1]}$ is changing, we take $u^{[1]}$ as an example to analyze the asymptotic properties of Solutions (12). In fact, $u^{[1]}$ and $v^{[1]}$ own the same curve characteristic lines.

Motivated by Refs. [40–42], we firstly perform the following asymptotic analysis procedure to investigate the asymptotic behaviors of $u^{[1]}$ in Solutions (12).

We firstly prove that the characteristic lines of $u^{[1]}$ are not the straight lines as follows:

We consider an arbitrary line $L : \frac{t}{\lambda_1} + c_1x = c_2$, where c_1 and c_2 are the arbitrary real numbers. Since $\rho = \lambda_1\theta - 8\beta\lambda_1^2x$, $u^{[1]}$ are dependent only on the variables θ and x . Thus, it is necessary to investigate the behavior of θ alone L as $|x| \rightarrow \infty$. In view of $\theta - \left(\frac{t}{\lambda_1} + c_1x\right) = (4\beta\lambda_1 - c_1)x$, as $x \rightarrow +\infty$, the value of θ is

$$\theta = \begin{cases} -\infty, & c_1 > 4\beta\lambda_1, \\ O(1) & c_1 = 4\beta\lambda_1, \\ +\infty, & c_1 < 4\beta\lambda_1, \end{cases} \tag{13}$$

and vice versa, where $O(1)$ denotes that the two quantities are of the same order, i.e., the ratio limit of two quantities tends to a nonzero constant.

As shown in Expressions (13), the value of θ can be $+\infty$, $-\infty$ or $O(1)$ at infinity on the line L . Hence, we can calculate the dominant behaviors of $u^{[1]}$ corresponding to the above three cases of θ as

$$u^{[1]} = \begin{cases} -2\frac{l_1(\rho + 2\lambda_1)}{\lambda_1^2 l_2} e^{\frac{\theta}{2}}, & \theta \rightarrow -\infty, \\ 2l_1 l_2 \frac{\left(l_1^2 e^{\frac{\theta}{2}} - l_2^2 e^{-\frac{\theta}{2}}\right)\rho - 2\lambda_1 \left(l_1^2 e^{\frac{\theta}{2}} + l_2^2 e^{-\frac{\theta}{2}}\right)}{l_1^2 l_2^2 \rho^2 + \lambda_1^2 (l_1^4 e^{\theta} + l_2^4 e^{-\theta}) + 2l_1^2 l_2^2 \lambda_1^2}, & \theta = O(1), \\ 2\frac{l_2(\rho - 2\lambda_1)}{\lambda_1^2 l_1} e^{-\frac{\theta}{2}}, & \theta \rightarrow +\infty. \end{cases} \tag{14}$$

Easy to know that $e^{\frac{\theta}{2}} \rightarrow 0$ as $\theta \rightarrow -\infty$, $e^{-\frac{\theta}{2}} \rightarrow 0$ as $\theta \rightarrow \infty$, and $l_1^2 l_2^2 \rho^2 \gg \left| \left(l_1^2 e^{\frac{\theta}{2}} - l_2^2 e^{-\frac{\theta}{2}} \right) \rho \right|$ as $\theta = O(1)$, $x \rightarrow \pm\infty$. That is to say, no matter which of the three cases in Expressions (13), $u^{[1]}$ will approach 0 as $|x| \rightarrow \infty$ alone the line L . In summary, characteristic lines of $u^{[1]}$ are not the straight lines.

Therefore, characteristic lines of $u^{[1]}$ are the curves in the $x - t$ plane. Along the curves to infinity, e^{θ} and ρ approach infinity. Thus, a balance between e^{θ} and ρ can be considered as

$$\frac{\rho}{e^{p\theta}} \sim O(1), \quad |x| \rightarrow +\infty, \tag{15}$$

where p is a real variable constant depending on the values of e^{θ} and ρ . According to the relationship between p and $\pm\frac{1}{2}$, we classify and obtain the following six dominant behaviors of $u^{[1]}$ as

$$u^{[1]} = \begin{cases} \frac{2l_1 e^{\frac{\theta}{2}}}{l_2 \rho}, & p > \frac{1}{2}, \theta \rightarrow \infty, \\ 2l_1 l_2 \frac{\rho e^{\frac{\theta}{2}}}{\lambda_1^2 l_1^2 e^{\theta} + l_2^2 \rho^2}, & p = \frac{1}{2}, \theta \rightarrow \infty, \\ \frac{2l_2 \rho}{l_1 \lambda_1^2 e^{\frac{\theta}{2}}}, & 0 < p < \frac{1}{2}, \theta \rightarrow \infty, \\ -\frac{2l_1 \rho}{l_2 \lambda_1^2 e^{-\frac{\theta}{2}}}, & -\frac{1}{2} < p < 0, \theta \rightarrow -\infty, \\ -2l_1 l_2 \frac{\rho e^{-\frac{\theta}{2}}}{\lambda_1^2 l_2^2 e^{-\theta} + l_1^2 \rho^2}, & p = -\frac{1}{2}, \theta \rightarrow -\infty, \\ -\frac{2l_2 e^{-\frac{\theta}{2}}}{l_1 \rho}, & p < -\frac{1}{2}, \theta \rightarrow -\infty. \end{cases} \tag{16}$$

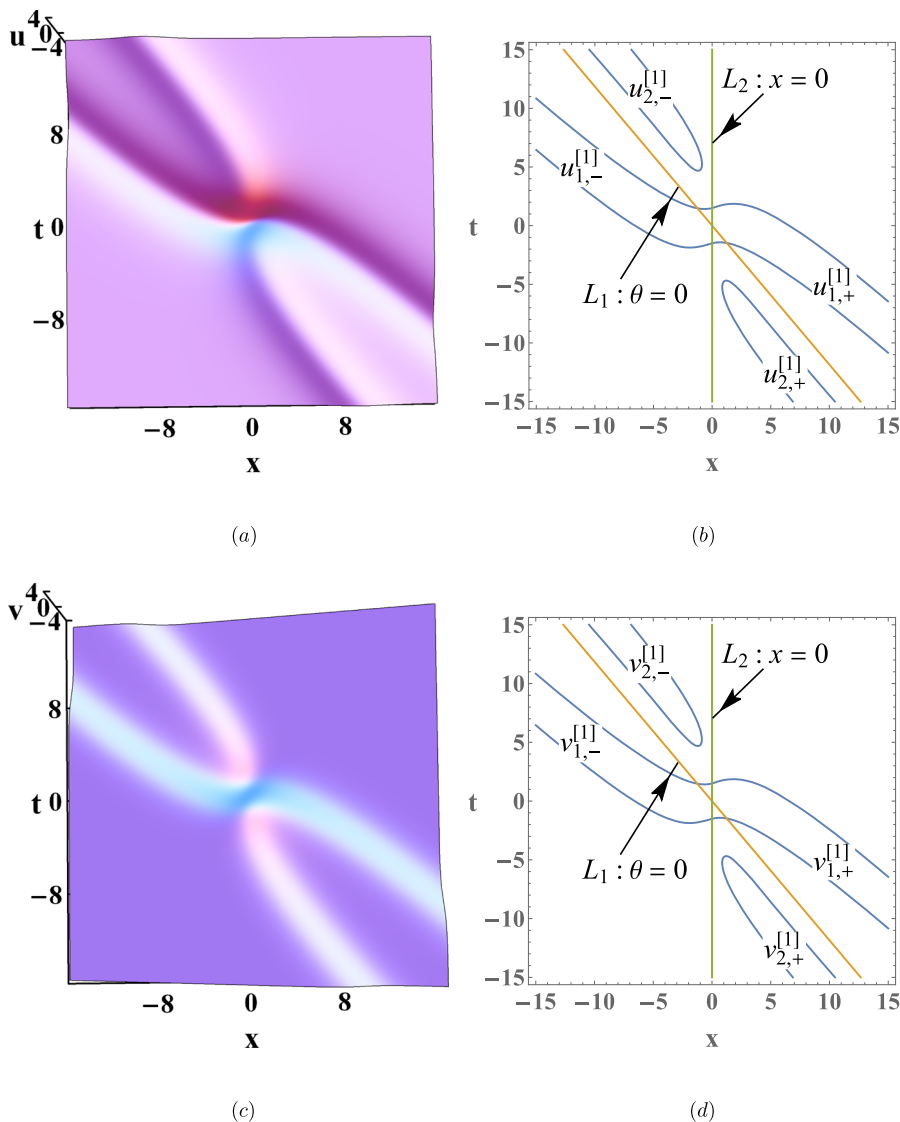
Equations (16) indicate that $u^{[1]}$ behaves as the solitons with the stable amplitudes only when $p = \pm\frac{1}{2}$. Whether $p = \frac{1}{2}$ or $-\frac{1}{2}$, x may approach to $+\infty$ or $-\infty$. Therefore, we assume that $\lambda_1 l_1 l_2 > 0$ and $\beta > 0$, and then calculate the following four asymptotic solitons as

$$\begin{aligned} u^{[1]} \rightarrow u_{1,+}^{[1]} &= \frac{1}{\lambda_1} \operatorname{sech}\left(\frac{\theta}{2} + \ln \frac{\lambda_1 l_1}{l_2 \rho}\right), \\ \rho e^{-\frac{\theta}{2}} &= O(1), \theta \rightarrow +\infty, x \rightarrow +\infty, \rho > 0, \\ u^{[1]} \rightarrow u_{1,-}^{[1]} &= \frac{1}{\lambda_1} \operatorname{sech}\left(\frac{\theta}{2} + \ln \frac{-\rho l_1}{\lambda_1 l_2}\right), \\ \rho e^{\frac{\theta}{2}} &= O(1), \theta \rightarrow -\infty, x \rightarrow -\infty, \rho < 0, \\ u^{[1]} \rightarrow u_{2,+}^{[1]} &= -\frac{1}{\lambda_1} \operatorname{sech}\left(\frac{\theta}{2} + \ln \frac{\rho l_1}{\lambda_1 l_2}\right), \\ \rho e^{\frac{\theta}{2}} &= O(1), \theta \rightarrow -\infty, x \rightarrow +\infty, \rho > 0, \\ u^{[1]} \rightarrow u_{2,-}^{[1]} &= -\frac{1}{\lambda_1} \operatorname{sech}\left(\frac{\theta}{2} + \ln \frac{\lambda_1 l_1}{-l_2 \rho}\right), \\ \rho e^{-\frac{\theta}{2}} &= O(1), \theta \rightarrow +\infty, x \rightarrow -\infty, \rho < 0. \end{aligned} \tag{17}$$

Similar to the above analysis procedure, we can prove that $v^{[1]}$ in Solutions (12) possesses the same characteristic lines as $u^{[1]}$ in Solutions (12). However, since the background of $v^{[1]}$ is a linear functions of t , i.e., βt , asymptotic solitons $v_{1,\pm}^{[1]}$ and $v_{2,\pm}^{[1]}$ have no fixed amplitudes.

3D figures and contour figures of $u^{[1]}$ and $v^{[1]}$ via Solutions (12) are shown in Fig. 2.

Fig. 2 a, c 3D figures; b, d Contour figures of the double-pole solitons via Solutions (12) with $\lambda_1 = 1$, $\beta = \frac{1}{4}$ and $l_{11} = l_{12} = 1$



Asymptotic Solitons (17) represent the two bright-type solitons $u_{1,\pm}^{[1]}$ and two dark-type solitons $u_{2,\pm}^{[2]}$. From Asymptotic Solitons (17), the following properties of the four asymptotic solitons $u_{1,\pm}^{[1]}$ and $u_{2,\pm}^{[1]}$ are obtained as follows:

(a) Amplitudes:

$$A(u_{1,\pm}^{[1]}) = A(u_{2,\pm}^{[1]}) = \frac{1}{|\lambda_1|}. \tag{18}$$

(b) Characteristic lines:

$$\begin{aligned} u_{1,+}^{[1]} : \lambda_1 l_1 e^{\frac{\theta}{2}} - l_2 \rho = 0; \quad u_{1,-}^{[1]} : \rho l_1 e^{\frac{\theta}{2}} + \lambda_1 l_2 = 0; \\ u_{2,+}^{[1]} : \rho l_1 e^{\frac{\theta}{2}} - \lambda_1 l_2 = 0; \quad u_{2,-}^{[1]} : \lambda_1 l_1 e^{\frac{\theta}{2}} + l_2 \rho = 0. \end{aligned} \tag{19}$$

(c) Slopes:

$$\begin{aligned} S(u_{1,\pm}^{[1]}) &= \frac{1}{4\lambda_1^2\beta} \frac{2\lambda_1 - |\rho|}{2\lambda_1 + |\rho|}; \\ S(u_{2,\pm}^{[1]}) &= \frac{1}{4\lambda_1^2\beta} \frac{2\lambda_1 + |\rho|}{2\lambda_1 - |\rho|}. \end{aligned} \tag{20}$$

(d) Phase shifts $P(\chi)$ between $u_{\chi,+}^{[1]}$ and $u_{\chi,-}^{[1]}$ ($\chi = 1, 2$):

$$P(1) = -P(2) = 2 \ln \left| \frac{\lambda_1}{\rho} \right|. \tag{21}$$

The above four asymptotic solitons own the same amplitude. In view of $P(1)$ and $P(2)$ are opposite under the same $|\rho|$, and the value of $S(u_{\lambda,+}^{[1]})$ at β is equal to that of $S(u_{\lambda,-}^{[1]})$ at $-\rho$, we can infer that the interaction between $u_1^{[1]}$ and $u_2^{[1]}$ is elastic.

We have

$$S(\theta) = -\frac{1}{4\lambda_1^2\beta} \leq S(u_{1,\pm}^{[1]}) \leq 0; \tag{22}$$

$$S(u_{2,\pm}^{[1]}) \leq S(\theta) = -\frac{1}{4\lambda_1^2\beta}.$$

Therefore, asymptotic solitons $u_{1,\pm}^{[1]}$ are located between the two straight lines $L_1 : \theta = 0$ and $L_2 : x = 0$, and asymptotic solitons $u_{2,\pm}^{[1]}$ are located outside of the straight line L_1 , as shown in Fig. 2b.

As we set $M = 1, r_1 = 2, N = 3$ in Solutions (9), the triple-pole solitons for Eq. (1) are illustrated in Fig. 3; as we set $M = 1, r_1 = 3, N = 4$ in Solutions (9), the quadruple-pole solitons for Eq. (1) are illustrated in Fig. 4. We summarize a rule about the N th-order multi-pole solitons for Eq. (1): when N is even, the N th-order multi-pole solitons consist of $\frac{N}{2}$ bright solitons and $\frac{N}{2}$ dark solitons; when N is odd, the N th-order multi-pole solitons consist of $\frac{N-1}{2}$ bright solitons and $\frac{N+1}{2}$ dark solitons. Moreover, these bright and dark solitons are arranged alternately.

Compared with the solitons in Refs. [8–19, 21, 22, 35], the double-pole solitons in Figs. 1 and 2 show

the different dynamic characteristics. Curve characteristic lines indicate that the velocities of the solitons are changing with the changes of x and t . Moreover, each branch of $u^{[1]}$ owns the same amplitude.

3.2 Interactions among the solitons and multi-pole solitons for System (1)

As we set $M = 1, r_1 = 0$ and $N = 1$ in Solutions (12), with respect to the magnetization related to the saturated ferromagnetic material and external magnetic field, expressions of the one-soliton solutions are derived as

$$u^{[1]} = -\frac{1}{\lambda_1} \operatorname{sech} \left(\frac{\theta}{2} + \ln \frac{l_{11}}{l_{12}} \right),$$

$$v^{[1]} = \beta x - \frac{l_{11}^2 e^\theta - l_{12}^2}{\lambda_1 (l_{11}^2 e^\theta + l_{12}^2)}, \tag{23}$$

$$\theta = \frac{t}{\lambda_1} + 4\beta\lambda_1 x.$$

From One-Soliton Solutions (23), we obtain that velocity of the one soliton is $-\frac{1}{4\beta\lambda_1^2}$.

As we set $M = 2, r_1 = 1, r_2 = 0$ and $N = 3$ in Solutions (12), the interaction among the one soliton and double-pole solitons is illustrated in Fig. 5. Figures 3 and 5 both contain three soliton components, including two curve-type solitons and one line-type soliton. However, the line-type soliton in Fig. 3 doesn't have a phase shift before and after the interaction while the line-type soliton in Fig. 5 has a phase shift before and after the interaction. In other

Fig. 3 3D figures of the triple-pole solitons: **a** Component u ; **b** Component v via Solutions (9) with $\lambda_1 = \frac{2}{3}, \beta = \frac{2}{3}$ and $l_{11} = l_{12} = 1$

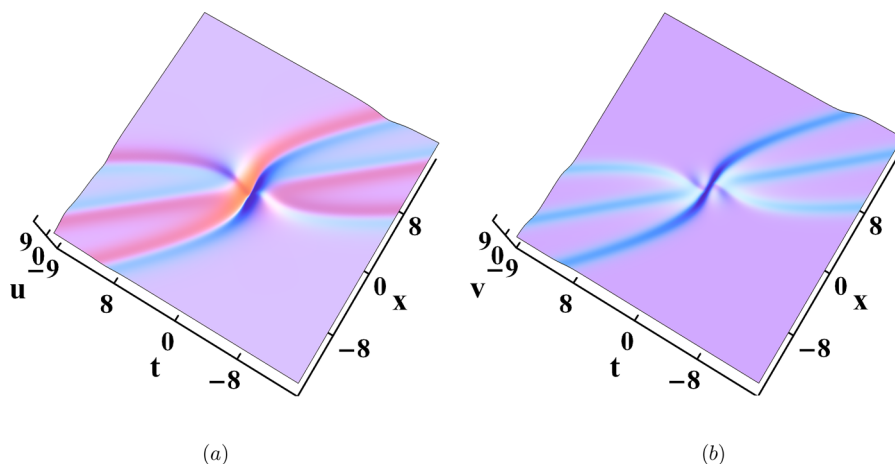


Fig. 4 3D figures of the quadruple-pole solitons: **a** Component u ; **b** Component v via Solutions (12) with $\lambda_1 = \frac{2}{3}$, $\beta = \frac{2}{3}$ and $l_{11} = l_{12} = 1$

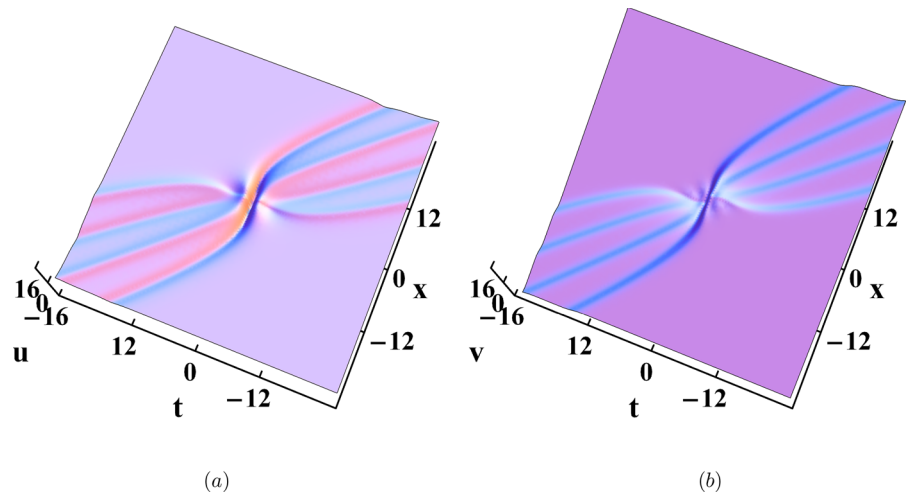
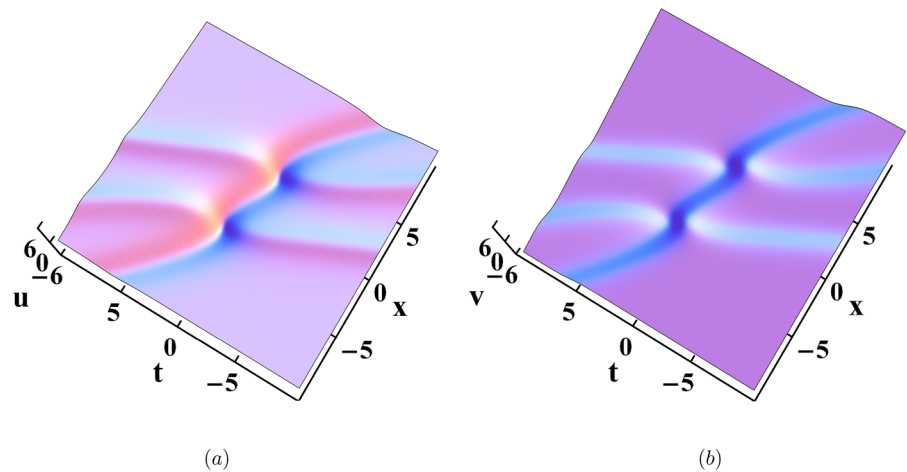


Fig. 5 3D figures of the interaction among the one soliton and double-pole solitons: **a** Component u ; **b** Component v via Solutions (12) with $\lambda_1 = \frac{2}{3}$, $\lambda_2 = -1$, $\beta = \frac{2}{3}$ and $l_{11} = l_{12} = l_{21} = l_{22} = 1$



words, we can consider that Fig. 3 with an arbitrary line-type soliton is a special case of Fig. 5.

As we set $M = 2$, $r_1 = 2$, $r_2 = 0$ and $N = 4$ in Solutions (12), the interaction among the one soliton and triple-pole solitons are illustrated in Fig. 6. As we set $M = 2$, $r_1 = 1$, $r_2 = 1$ and $N = 4$ in Solutions (12), the interaction among the two double-pole solitons are illustrated in Fig. 7.

Compared with those simple situations in Figs. 1, 3, 4, the interaction areas in Figs. 5, 6, 7 appear more disordered, which correspond to the realistic occasions of the electromagnetic wave propagation in a ferromagnetic saturator. In fact, with the increase of M and N , i.e., the total order of Solutions (12) and the number of spectral parameters, solutions of System (1) will be composed of more solitons. Due to the limitation of

computing power, we only show up to the fourth-order solutions.

In Figs. 5, 6, 7, all the solitons extend to infinity and maintain their shapes. We find that before and after the interaction, the solitons and multi-pole solitons only have a phase shift while their velocities, amplitudes, shapes, and widths do not change at all. That is to say, interactions among the solitons and multi-pole solitons are elastic. We also find that the one soliton component in Fig. 6 is dark-type, while the one soliton component in Fig. 5 is bright-type.

In Figs. 1, 2, 3, 4, only a peak arises in the multi-pole solitons. However, soliton interactions in Figs. 5, 6, 7 present more peaks and depressions as follows: two depressions in Fig. 5, two peaks and a depression in Fig. 6, and two peaks and two depressions in Fig. 7.

Fig. 6 3D figures of the interaction among the one soliton and triple-pole solitons: **a** Component u ; **b** Component v via Solutions (12) with $\lambda_1 = \frac{2}{3}$, $\lambda_2 = -1$, $\beta = \frac{2}{3}$ and $l_{11} = l_{12} = l_{21} = l_{22} = 1$

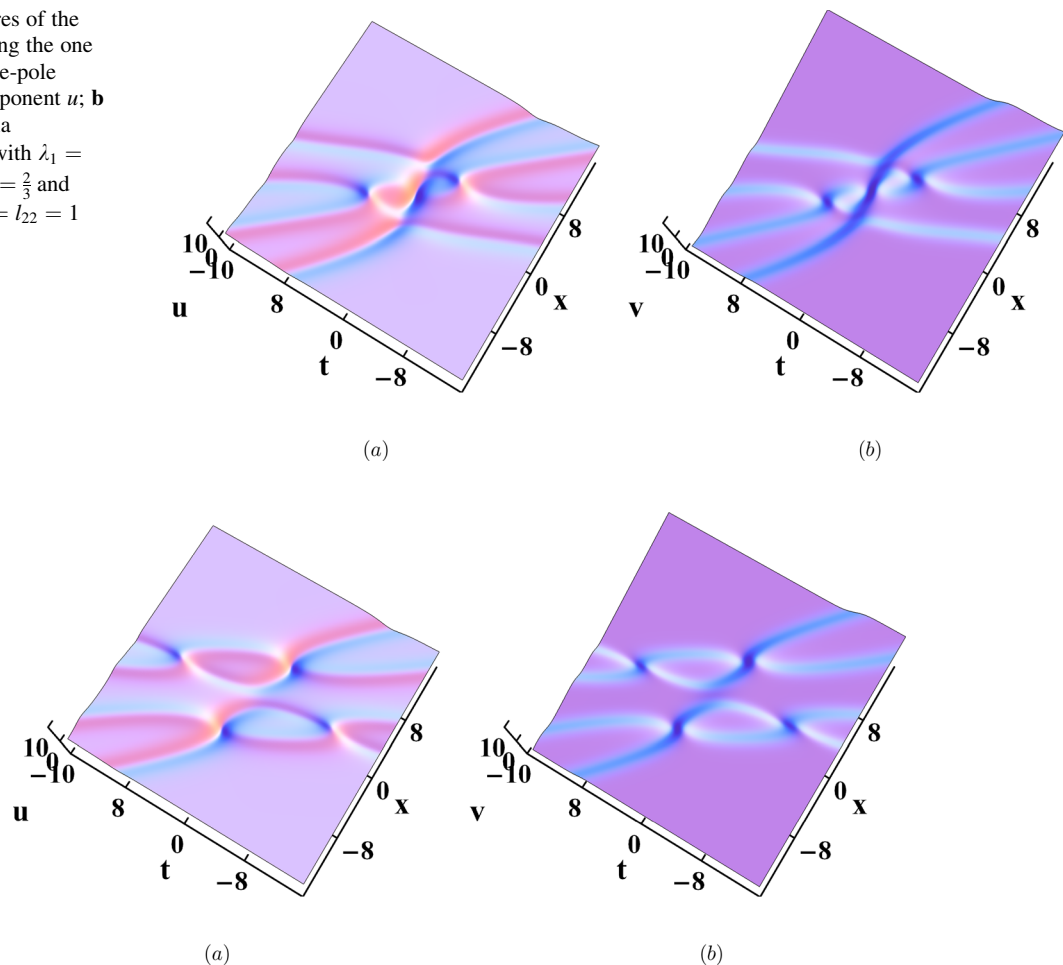


Fig. 7 3D figures of the interaction among the two double-pole solitons: **a** Component u ; **b** Component v via Solutions (12) with $\lambda_1 = \frac{2}{3}$, $\lambda_2 = -1$, $\beta = \frac{2}{3}$ and $l_{11} = l_{12} = l_{21} = l_{22} = 1$

Moreover, interaction regions of the fourth-order solitons in Figs. 6, 7 are kinked.

It has been reported that the bound-state solitons appear and exhibit the periodic attractions or repulsions between the adjacent solitons when two or more solitons have the same velocity [43]. However, in Solutions (12), unequal spectral parameters indicate that different solitons have different velocities, thus, bound-state solitons cannot be derived.

4 Conclusions

In this paper, a Kraenkel-Manna-Merle system, i.e., System (1), which describes the nonlinear

electromagnetic short waves in a ferromagnetic saturator, has been investigated. On the basis of N -Fold DT (6), a GDT has been constructed and utilized to derive Solutions (12).

Double-pole soliton solutions have been derived as Solutions (12) and have been shown in Fig. 1. Asymptotic analysis on Solutions (12) has given rise to Asymptotic Solitons (17), which lead to Characteristic Lines (19), Slopes (20) and Phase Shifts (21) of $u_{1,\pm}^{[1]}$ and $u_{2,\pm}^{[1]}$. We have found that the four asymptotic solitons $u_{1,\pm}^{[1]}$ and $u_{2,\pm}^{[1]}$ own the same amplitude $|\lambda_1|^{-1}$, the asymptotic solitons $u_{1,\pm}^{[1]}$ are located between the two straight lines L_1 and L_2 , and the asymptotic

solitons $u_{2,\pm}^{[1]}$ are located outside of the straight line L_1 , as shown in Fig. 2. The above conclusions and phenomena on the double-pole solitons have been similar to those analyses in Refs. [38, 40], i.e., System (1) and the generalized nonlinear Schrödinger equations have shown the same multi-pole soliton characteristics.

For Eq. (1), the triple-pole solitons have been shown in Fig. 3; the quadruple-pole solitons have been illustrated in Fig. 4; the interaction among the one soliton and double-pole solitons has been presented in Fig. 5; the interaction among the one soliton and triple-pole solitons has been shown in Fig. 6; the interaction among the two double-pole solitons has been presented in Fig. 7. We have summarized a rule about the N th-order multi-pole solitons: when N is even, the N th-order multi-pole solitons consists of $\frac{N}{2}$ bright solitons and $\frac{N}{2}$ dark solitons; when N is odd, the N th-order multi-pole solitons consists of $\frac{N-1}{2}$ bright solitons and $\frac{N+1}{2}$ dark solitons. Compared with the normal solitons in Ref. [33], the above multi-pole solitons have only shown changes in propagation velocities while other physical properties such as the wave heights and amplitudes remain unchanged.

In the future, we expect to extend the above asymptotic analysis method to the triple-pole or even N -fold-pole soliton solutions and multi-pole breather solutions, although those discussions must be more complex. It is worth noting that the simultaneous emergence among the multi-pole phenomena and bound states also have potential research spaces.

Funding We have expressed our sincere thanks to the Editors and Reviewers for their valuable comments. This work has been supported by the National Natural Science Foundation of China under Grant No. 11772017.

Data availability Data sharing not applicable to this article as no datasets were generated or analysed during the current study.

Declarations

Conflict of interest The authors declare that they have no conflict of interest.

References

1. Yang, J.Q., Zhou, Y., Han, S.T.: Functional applications of future data storage devices. *Adv. Electron. Mater.* **7**, 2001181 (2021)
2. Walter, J., Voigt, B., Day-Roberts, E., Heltemes, K., Fernandes, R.M., Birol, T., Leighton, C.: Voltage-induced ferromagnetism in a diamagnet. *Sci. Adv.* **6**, eabb7721 (2020)
3. Nevirkovets, I.P., Mukhanov, O.A.: Memory cell for high density arrays based on a multiterminal superconducting ferromagnetic device. *Phys. Rev. Appl.* **10**, 034013 (2018)
4. Davidson, A., Amin, V.P.P., Aljuaid, W.S., Haney, P.M., Fan, X.: Perspectives of electrically generated spin currents in ferromagnetic materials. *Phys. Lett. A* **384**, 126228 (2020)
5. Barman, A., Sinha, J.: *Spin Dynamics and Damping in Ferromagnetic Thin Films and Nanostructures*. Springer, Cham (2018)
6. Goldman, A.: *Modern Ferrite Technology*. Springer, New York (1993)
7. Kraenkel, R.A., Manna, M.A., Merle, V.: Nonlinear short wave propagation in ferrites. *Phys. Rev. E* **61**, 976 (2000)
8. Jin, X.W., Lin, J.: Rogue wave, interaction solutions to the KMM system. *J. Magn. Magn. Mater.* **502**, 166590 (2020)
9. Younas, U., Sulaiman, T.A., Yusuf, A., Bilal, M., Younis, M., Rehman, S.U.: New solitons and other solutions in saturated ferromagnetic materials modeled by Kraenkel–Manna–Merle system. *Indian J. Phys.* **96**, 181 (2021)
10. Li, B.Q., Ma, Y.L.: Loop-like periodic waves and solitons to the Kraenkel–Manna–Merle system in ferrites. *J. Electromagn. Wave. Appl.* **32**, 1275 (2018)
11. Tchokouansi, H.T., Tchidjo, R.T., Felenou, E.T., Kuetche, V.K.: Propagation of magnetic solitary waves in inhomogeneous ferrites, subjected to damping effects. *J. Magn. Magn. Mater.* **554**, 169281 (2022)
12. Nguepjou, F.T., Kuetche, V.K., Kofane, T.C.: Soliton interactions between multivalued localized waveguide channels within ferrites. *Phys. Rev. E* **89**, 063201 (2014)
13. Tchokouansi, H.T., Kuetche, V.K., Kofane, T.C.: On the propagation of solitons in ferrites: the inverse scattering approach. *Chaos Solitons Fract.* **86**, 64 (2016)
14. Ma, Y.L., Li, B.Q.: Kraenkel–Manna–Merle saturated ferromagnetic system: Darboux transformation and loop-like soliton excitations. *Chaos Solitons Fract.* **159**, 112179 (2022)
15. Li, B.Q., Ma, Y.L.: Rich soliton structures for the Kraenkel–Manna–Merle (KMM) system in ferromagnetic materials. *J. Supercond. Nov. Magn.* **31**, 1773 (2018)
16. Rehman, S.U., Bilal, M., Ahmad, J.: Dynamics of soliton solutions in saturated ferromagnetic materials by a novel mathematical method. *J. Magn. Magn. Mater.* **538**, 168245 (2021)
17. Si, H.L., Li, B.Q.: Two types of soliton twinning behaviors for the Kraenkel–Manna–Merle system in saturated ferromagnetic materials. *Optik* **166**, 49 (2018)

18. Li, B.Q., Ma, Y.L., Sathishkumar, P.: The oscillating solitons for a coupled nonlinear system in nanoscale saturated ferromagnetic materials. *J. Magn. Magn. Mater.* **474**, 661 (2019)
19. Younas, U., Bilal, M., Ren, J.: Diversity of exact solutions and solitary waves with the influence of damping effect in ferrites materials. *J. Magn. Magn. Mater.* **549**, 168995 (2022)
20. Tchidjo, R.T., Tchokouansi, H.T., Felenou, E.T., Kuetche, V.K., Bouetou, T.B.: Influence of damping effects on the propagation of magnetic waves in ferrites. *Chaos Solitons Fract.* **119**, 203 (2019)
21. Tchokouansi, H.T., Felenou, E.T., Tchidjo, R.T., Kuetche, V.K., Bouetou, T.B.: Traveling magnetic wave motion in ferrites: impact of inhomogeneous exchange effects. *Chaos Solitons Fract.* **121**, 1 (2019)
22. Arshed, S., Raza, N., Butt, A.R., Akgül, A.: Exact solutions for Kraenkel–Manna–Merle model in saturated ferromagnetic materials using β -derivative. *Phys. Scr.* **96**, 124018 (2021)
23. Li, B.Q., Ma, Y.L.: Oscillation roguewaves for the Kraenkel–Manna–Merle system in ferrites. *J. Magn. Magn. Mater.* **537**, 168182 (2021)
24. Yang, D.Y., Tian, B., Tian, H.Y., Wei, C.C., Shan, W.R., Jiang, Y.: Darboux transformation, localized waves and conservation laws for an M-coupled variable-coefficient nonlinear Schrödinger system in an inhomogeneous optical fiber. *Chaos Solitons Fract.* **156**, 111719 (2022)
25. Cheng, C.D., Tian, B., Shen, Y., Zhou, T.Y.: Bilinear form and Pfaffian solutions for a (2+1)-dimensional generalized Konopelchenko–Dubrovsky–Kaup–Kupershmidt system in fluid mechanics and plasma physics. *Nonlinear Dyn.* **111**, 6659–6675 (2023)
26. Zhou, T.Y., Tian, B.: Auto-Bäcklund transformations, Lax pair, bilinear forms and bright solitons for an extended (3+1)-dimensional nonlinear Schrödinger equation in an optical fiber. *Appl. Math. Lett.* **133**, 108280 (2022)
27. Cheng, C.D., Tian, B., Ma, Y.X., Zhou, T.Y., Shen, Y.: Pfaffian, breather and hybrid solutions for a (2+1)-dimensional generalized nonlinear system in fluid mechanics and plasma physics. *Phys. Fluids* **34**, 115132 (2022)
28. Li, L., Pang, L., Wang, R., Zhang, X., Hui, Z., Han, D., Zhao, F.L.: Ternary transition metal dichalcogenides for high power vector dissipative soliton ultrafast fiber laser. *Laser Photon. Rev.* **16**, 2100255 (2022)
29. Gao, X.Y., Guo, Y.J., Shan, W.R.: Reflecting upon some electromagnetic waves in a ferromagnetic film via a variable-coefficient modified Kadomtsev–Petviashvili system. *Appl. Math. Lett.* **132**, 108189 (2022)
30. Bilal, M., Ahmad, J.: Dynamics of soliton solutions in saturated ferromagnetic materials by a novel mathematical method. *J. Magn. Magn. Mater.* **538**, 168245 (2021)
31. Liu, F.Y., Gao, Y.T., Yu, X., Ding, C.C.: Wronskian, Gramian, Pfaffian and periodic-wave solutions for a (3+1)-dimensional generalized nonlinear evolution equation arising in the shallow water waves. *Nonlinear Dyn.* **108**, 1599–1616 (2022)
32. Feng, C.H., Tian, B., Yang, D.Y., Gao, X.T.: Lump and hybrid solutions for a (3+1)-dimensional Boussinesq-type equation for the gravity waves over a water surface. *Chin. J. Phys.* (2023). <https://doi.org/10.1016/j.cjph.2023.03.023>
33. Zhou, T.Y., Tian, B., Chen, Y.Q., Shen, Y.: Painlevé analysis, auto-Bäcklund transformation and analytic solutions of a (2+1)-dimensional generalized Burgers system with the variable coefficients in a fluid. *Nonlinear Dyn.* **108**, 2417–2428 (2022)
34. Shen, Y., Tian, B., Liu, S.H., Zhou, T.Y.: Studies on certain bilinear form, N-soliton, higher-order breather, periodic-wave and hybrid solutions to a (3+1)-dimensional shallow water wave equation with time-dependent coefficients. *Nonlinear Dyn.* **108**, 2447–2460 (2022)
35. Shen, Y., Tian, B., Zhou, T.Y., Gao, X.T.: N-fold Darboux transformation and solitonic interactions for the Kraenkel–Manna–Merle system in a saturated ferromagnetic material. *Nonlinear Dyn.* **111**, 2641–2649 (2023)
36. Wu, X.H., Gao, Y.T., Yu, X., Ding, C.C., Liu, F.Y., Jia, T.T.: Darboux transformation, bright and dark-bright solitons of an N-coupled high-order nonlinear Schrödinger system in an optical fiber. *Mod. Phys. Lett. B* **36**, 2150568 (2022)
37. Wu, X.H., Gao, Y.T., Yu, X., Ding, C.C.: Vector breathers, rogue and breather-rogue waves for a coupled mixed derivative nonlinear Schrödinger system in an optical fiber. *Nonlinear Dyn.* **111**, 5641 (2023)
38. Wang, M., Chen, Y.: General multi-soliton and higher-order soliton solutions for a novel nonlocal Lakshmanan–Porsezian–Daniel equation. *Nonlinear Dyn.* **111**, 655 (2023)
39. Wang, M., Chen, Y.: Dynamic behaviors of mixed localized solutions for the three-component coupled Fokas–Lenells system. *Nonlinear Dyn.* **98**, 1781 (2019)
40. Lin, M., Yue, X., Xu, T.: Multi-pole solutions and their asymptotic analysis of the focusing Ablowitz–Ladik equation. *Phys. Scr.* **95**, 055222 (2020)
41. Lin, M., Zhang, X., Xu, T., Ling, L.: Asymptotic analysis and soliton interactions of the multi-pole solutions in the Hirota equation. *J. Phys. Soc. Jpn.* **89**, 054004 (2020)
42. Xu, T., Lan, S., Li, M., Li, L.L., Zhang, G.W.: Mixed soliton solutions of the defocusing nonlocal nonlinear Schrödinger equation. *Phys. D* **47**, 390 (2019)
43. Wu, X.H., Gao, Y.T., Yu, X., Ding, C.C., Li, L.Q.: Modified generalized Darboux transformation, degenerate and bound-state solitons for a Lakshmanan–Porsezian–Daniel equation. *Chaos Solitons Fract.* **162**, 112399 (2022)
44. Gao, X.T., Tian, B., Shen, Y., Feng, C.H.: Considering the shallow water of a wide channel or an open sea through a generalized (2+1)-dimensional dispersive long-wave system. *Qual. Theory Dyn. Syst.* **21**, 104 (2022)
45. Gao, X.Y., Guo, Y.J., Shan, W.R.: Symbolically computing the shallow water via a (2+1)-dimensional generalized modified dispersive water-wave system: similarity reductions, scaling and hetero-Bäcklund transformations. *Qual. Theory Dyn. Syst.* **22**, 17 (2023)
46. Liu, F.Y., Gao, Y.T.: Lie group analysis for a higher-order Boussinesq–Burgers system. *Appl. Math. Lett.* **132**, 108094 (2022)
47. Yang, D.Y., Tian, B., Hu, C.C., Liu, S.H., Shan, W.R., Jiang, Y.: Conservation laws and breather-to-soliton transition for a variable-coefficient modified Hirota equation in an inhomogeneous optical fiber. *Wave. Random Complex* (2023). <https://doi.org/10.1080/17455030.2021.1983237>

48. Gao, X.T., Tian, B.: Water-wave studies on a (2+1)-dimensional generalized variable-coefficient Boiti-Leon-Pempinelli system. *Appl. Math. Lett.* **128**, 107858 (2022)

Publisher's Note Springer Nature remains neutral with regard to jurisdictional claims in published maps and institutional affiliations.

Springer Nature or its licensor (e.g. a society or other partner) holds exclusive rights to this article under a publishing agreement with the author(s) or other rightsholder(s); author self-archiving of the accepted manuscript version of this article is solely governed by the terms of such publishing agreement and applicable law.